

## Full Length Article

## Flexible carbon capture using MOF fixed bed adsorbers at an NGCC plant

Mahpara Habib<sup>a</sup>, Aaron M. Esquino<sup>a</sup>, Ryan Hughes<sup>b</sup>, Frits Byron Soepyan<sup>c</sup>, Leo R. Nemetz<sup>d</sup>, Zhien Zhang<sup>b</sup>, Md Emdadul Haque<sup>b</sup>, David R. Luebke<sup>c</sup>, G. Glenn Lipscomb<sup>d</sup>, Michael S. Matuszewski<sup>c</sup>, Debansu Bhattacharyya<sup>b</sup>, Katherine M. Hornbostel<sup>a,\*</sup>

<sup>a</sup> Department of Mechanical Engineering and Materials Science, University of Pittsburgh, Pittsburgh, PA 15213, USA

<sup>b</sup> Department of Chemical and Biomedical Engineering, West Virginia University, Morgantown, WV 26506, USA

<sup>c</sup> AristoSys, LLC, 2400 Ansys Drive, Suite 102, Canonsburg, PA 15317, USA

<sup>d</sup> Department of Chemical Engineering, University of Toledo, Toledo, OH 43606, USA



## ARTICLE INFO

## Keywords:

NGCC carbon capture

Hybrid carbon capture system

Direct air capture

Metal-organic framework carbon capture

Fixed bed adsorber modeling

## ABSTRACT

Novel carbon capture systems are necessary to help natural gas power plants approach net zero CO<sub>2</sub> emissions. We propose a hybrid carbon capture system attached to a natural gas combined cycle (NGCC) power plant that consists of a membrane system and a solid sorbent system, with this work focusing on the design of the solid sorbent system. We modeled fixed bed adsorbers that are packed with metal-organic framework (MOF) solid sorbents that adsorb CO<sub>2</sub> and undergo temperature swing desorption using steam from the power plant. Parametric simulation of adsorber conditions showed that ten 5-m diameter beds adsorbing in parallel with 4.9 bars inlet gas pressure and 1.5 bars of steam pressure at a flow rate of 0.15 kmol/s led to optimized performance. This study enabled us to determine that the MOF bed adsorber can attain 86.6 % and 85.4 % carbon capture during peak and off-peak operation, respectively. When combined with the membrane capture system, this results in overall capture rates of 98.4 % and 98.9 % during peak and off-peak operation, respectively. Although we were unable to attain net-zero or net-negative emissions in this study, we are confident that net-negative operation could be obtained in future work by selecting a solid sorbent better suited to direct air capture conditions so that more air could be processed by the solid sorbent system.

## Tweetable abstract

This work optimized a metal-organic framework (MOF) solid sorbent system used in combination with membrane carbon capture at a natural gas (NGCC) power plant and found that greater than 98 % carbon capture could be attained.

## 1. Introduction

CO<sub>2</sub> concentration in the atmosphere has risen from 280 ppm to approximately 418 ppm due to the increased use of fossil fuels following the Industrial Revolution (Kiani et al., 2020; Hashemi et al., 2022). This is cause for concern because CO<sub>2</sub> is a major greenhouse gas and is the primary cause of global warming (Shi et al., 2020; Hansen et al., 2010; Lenssen et al., 2019). A way to address this concern is by devising methods to capture CO<sub>2</sub> from power plant flue gas, i.e. post-combustion capture. For example, He et al. investigated the scheduling and optimization of a MEA-solvent based carbon capture plant that was integrated

with an NGCC power plant to clean up its exhaust (He and Ricardez-Sandoval, 2016). Diego et al. studied the integration of a hybrid capture system that consisted of a CO<sub>2</sub> selective membrane and an amine scrubbing plant with an NGCC power plant (Diego et al., 2018). While certain power production and manufacturing industries have devised point-source carbon capture systems to reduce the amount of CO<sub>2</sub> they release into the air, post-combustion capture is not yet feasible for other major CO<sub>2</sub> producing sectors, such as the transportation industry, which accounts for nearly 50 % of greenhouse gas emissions (Seipp et al., 2017; Lackner et al., 2012; Choi et al., 2011). Therefore, to mitigate global warming long-term, we must also implement negative emissions technologies, such as direct air capture, to offset difficult-to-abate long-term CO<sub>2</sub> emissions.

While using fossil fuels as the energy source for running direct air capture (DAC) may seem contradictory, it will be expensive and impractical to power DAC using renewable sources alone, as this will require massive land space and capital cost. Coupling DAC with fossil fuels could also enable rapid scale-up by leveraging existing infrastructure, and reduce operating costs by taking advantage of the electricity, steam, and

\* Corresponding author.

E-mail address: [hornbostel@pitt.edu](mailto:hornbostel@pitt.edu) (K.M. Hornbostel).

<https://doi.org/10.1016/j.ccst.2023.100170>

Received 29 September 2023; Received in revised form 21 November 2023; Accepted 22 November 2023

2772-6568/© 2023 The Authors. Published by Elsevier Ltd on behalf of Institution of Chemical Engineers (IChemE). This is an open access article under the CC BY-NC-ND license (<http://creativecommons.org/licenses/by-nc-nd/4.0/>)

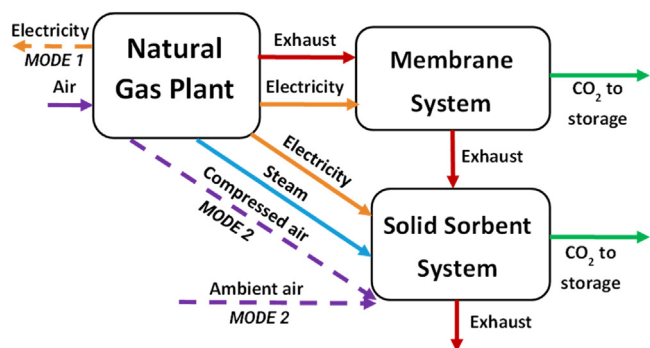


**Fig. 1.** The integrated system consists of a natural gas (NGCC) power plant with two carbon capture systems: membranes and solid sorbents. The solid sorbent system (the focus of this paper) operates downstream of the membrane system. During Mode 1 (normal operation), the solid sorbent just captures CO<sub>2</sub> from the membrane exhaust. During Mode 2 (off-peak operation), where the NGCC plant does not send electricity to the grid and the solid sorbent system captures CO<sub>2</sub> from air in addition to the membrane exhaust. This air can come from compressed air extracted from the natural gas compressor and/or ambient air from the surroundings. If the CO<sub>2</sub> in the solid sorbent system exhaust is < 400 ppm, then the overall system is performing negative emissions in Mode 2.

compressed air from the power plant. The FLECCS (FLExible Carbon Capture and Storage) program under ARPA-E was designed to investigate how to leverage fossil fuels to perform DAC and other beneficial functions long-term. Research conducted under this program included work by Realf et al. (2021), which proposed combining an NGCC power plant with an amine scrubbing plant and a modular DAC system. Another project funded by this program was led by Herzog et al., which involved capturing CO<sub>2</sub> from flue gas from a power plant using a calciner along with a lime-based DAC system (Sheha et al., 2021). The research presented in this paper, which is also a part of the FLECCS program, proposes the use of a hybrid membrane + solid sorbent carbon capture system retrofitted to an NGCC power plant. This is a novel concept that proposes operating the NGCC power plant during off-peak hours (when the plant would normally power down) to perform direct air capture in the solid sorbent fixed bed system. The hybrid carbon capture system will thus capture CO<sub>2</sub> from both the power plant exhaust and from the air. The membrane system is upstream of the solid sorbent system and acts as the primary point-source carbon capture system, while the sorbent system captures both CO<sub>2</sub> from the membrane exhaust and CO<sub>2</sub> from the air. Thus, the hybrid carbon capture system is not only designed to perform high levels of carbon capture, but it is also adaptable to changes in the grid. Alptekin et al. from TDA Research have previously developed and successfully pilot-tested a hybrid membrane-sorbent system for post-combustion capture from large-scale CO<sub>2</sub> emitters such as refineries and coal power plants (Gribble et al., 2022; Alptekin, 2020). Our work builds on this concept and takes it a step further to perform direct air capture in addition to point source capture during off-peak hours.

Note that the scope of this paper only involves the design and simulation of the fixed bed adsorber system, since the MTR membrane used in our system has already been extensively modeled and studied for NGCC capture (Merkel et al., 2010; Baker et al., 2017; Merkel et al., 2012). Fig. 1 below illustrates Modes 1 and 2 for our integrated system at a high level. During Mode 1 (normal operation), the NGCC plant sends electricity to the grid, and the hybrid carbon capture system simply captures CO<sub>2</sub> from the NGCC exhaust. For the solid sorbent system, this means that it only needs to process the membrane exhaust during Mode 1. During Mode 2 operation (off-peak operation), the NGCC plant no longer sends electricity to the grid, and only operates to power the carbon capture systems. During Mode 2, the solid sorbent beds remove CO<sub>2</sub> from both the membrane exhaust and from air. This air can come

from a combination of ambient air and compressed air extracted from the natural gas compressor. Extracted compressed air from the gas turbine (GT) compressor improves partial pressure of CO<sub>2</sub> and therefore, can improve the loading of the DAC sorbent. Air extraction from the GT compressor has been reported in the existing literature (Igie et al., 2021; Abudu et al., 2020; Yang et al., 2020). Maximum extraction flow rate and pressure of the extracted air vary depending on the extraction stage of the GT compressor and make and model of the GT. In Mode 2 of our system, a portion of air before entering the solid sorbent capture system is extracted from the compressor in the gas turbine (GT) in the NGCC plant. It provides high-pressure air mixed with membrane capture system exhaust gas for the adsorption system to achieve the net-zero capture.

The membrane system enables rapid response times, while the sorbent system enables higher carbon capture rates. The proposed system could theoretically achieve net-zero or even net-negative CO<sub>2</sub> emissions overall if Mode 2 operates often enough and removes enough CO<sub>2</sub> from the air to offset CO<sub>2</sub> emissions during Mode 1. A more detailed process flow diagram of this integrated system is given in the Supplementary Information (Fig. SI1), and a pending publication from our group will delve into integrated system level optimization (Soeptyan et al., 2024).

We selected solid sorbents instead of aqueous solvents for our adsorbers because solid sorbents generally need lower energy and operating cost to run and can better handle low CO<sub>2</sub> concentration capture (Keith et al., 2018; Sadiq et al., 2020). The solid sorbent selected for our system must be able to capture CO<sub>2</sub> under conditions ranging from NGCC exhaust (~40,000 ppm CO<sub>2</sub>) to unpressurized air (~400 ppm CO<sub>2</sub>). It was also important to select a sorbent that can withstand humid conditions and use steam for temperature swing desorption (since steam is abundant in NGCC plants). Metal-organic frameworks (MOFs) are a type of solid sorbent that consist of metal ions linked to an organic ligand and that can adsorb gases selectively. Several MOFs have demonstrated high selectivity towards CO<sub>2</sub>, and can be used for carbon capture in both post-combustion and direct air capture scenarios (Millward and Yaghi, 2005; Li et al., 2009). For example, Sinha et al. investigated the adsorptive performance of two MOFs, MIL-101(Cr)-PEI-800 and mmen-Mg<sub>2</sub>(dobpdc), for direct air capture, and found that the latter was favorable because of its lower energy requirements (Sinha et al., 2017). McDonald et al. found that mmen-Mg<sub>2</sub>(dobpdc) has a CO<sub>2</sub> adsorption capacity of 2.0 mmol/g at 0.39 bars and 25 °C and 3.14 mmol/g at 0.15 bars and 40 °C, and is thus an excellent sorbent for both direct air capture and post-combustion capture conditions (McDonald et al., 2012).

Since our carbon capture system is retrofitted to a NGCC power plant and captures CO<sub>2</sub> from power plant exhaust as well as air, we selected a solid sorbent that can capture CO<sub>2</sub> over that wide range of conditions. More specifically, we selected a tetraamine-appended Mg<sub>2</sub>(dobpdc)(3-4-3) MOF material recently developed by Dr. Jeffrey Long's group at UC Berkeley (Kim et al., 2020). This MOF material has a high breakthrough capacity of 2.0 ± 0.2 mmol/g at 100 °C under humid conditions and a 90 % CO<sub>2</sub> capture rate for natural gas exhaust (Kim et al., 2020). Their MOF has differential adsorption enthalpy ( $\Delta h_{ads}$ ) and entropy ( $\Delta s_{ads}$ ) values of 99 ± 3 kJ/mol and 223 ± 8 J/mol·K, respectively, at a loading of 1 mmol CO<sub>2</sub>/g (Kim et al., 2020). This high adsorption enthalpy indicates that this MOF is capable of adsorption at high temperatures, resulting in a smaller temperature swing between adsorption and desorption (resulting in lower operating costs). This tetraamine-appended MOF is also stable in the presence of humidity over 1000 cycles and can be regenerated using low-grade steam (~120 °C), which could potentially leverage the steam infrastructure of a NGCC plant. While this sorbent has been proposed as an excellent sorbent for post-combustion capture of natural gas, it was also shown to be capable of adsorbing CO<sub>2</sub> at lower concentrations, thus making it a potential sorbent for a direct air capture system. In addition to that, the unique dual-step shape of its isotherms can be exploited in our process-level design.

The scope of this paper covers the design of the solid sorbent carbon capture system. First we describe our efforts to model the isotherms of

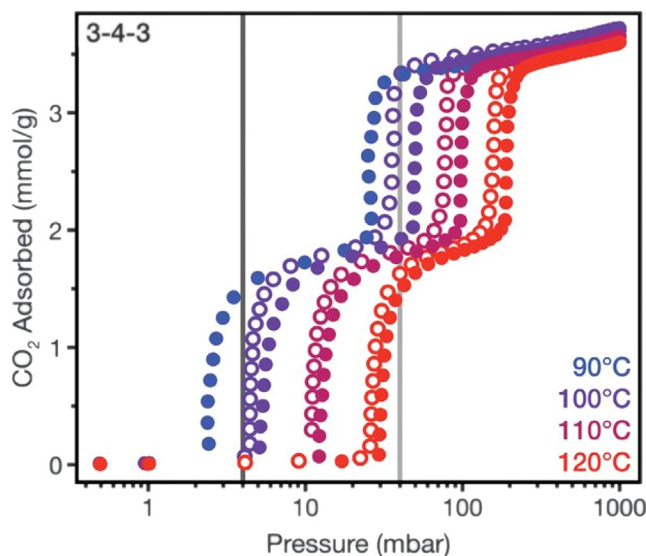


Fig. 2. Experimental isotherm data for the  $\text{Mg}_2(\text{dobpdc})(3-4-3)$  MOF material selected for our model, where filled circles denote adsorption isotherms and open circles denote desorption isotherms. Figure reproduced with permission from Kim et al. (2020).

the tetraamine-appended MOF used in our fixed bed adsorber model (Section 2.1). Next, we describe our MOF fixed bed adsorber model setup and governing equations (Section 2.2). Next, we present the results of simulations that we ran to determine the optimal adsorber bed design and operating conditions (Section 3.1). Then we present the results for Mode 1 & Mode 2 operation of our optimized adsorber beds (Section 3.2). Finally, we investigate the impact of adding excess ambient air to our adsorber bed during Mode 2 (Section 3.3) and discuss our conclusions (Section 4).

## 2. Methodology

### 2.1. Isotherm modeling

To the best of our knowledge, no model exists that describes the isotherm behavior of the tetraamine-appended  $\text{Mg}_2(\text{dobpdc})$  MOF material. The experimental adsorption isotherm data for this MOF material, for temperatures ranging between 90 and 120 °C, is shown below in Fig. 2 (reproduced with permission from Kim et al. 2020). Its dual-step adsorption curve does not fit the traditional single-step isotherm models. However, several isotherm models exist that may be modified and adapted to fit this unique double-step shaped isotherm (Hefti et al., 2016; Kundu et al., 2018; Pai et al., 2019; Bao et al., 2011; Hughes et al., 2021). Of these isotherm models, Hughes et al. determined that the Dual-site Sips isotherm model could be fitted to a close degree to the step-shaped isotherms of a similar MOF material developed by the same research group (Hughes et al., 2021; Siegelman et al., 2019). Due to the similarities in structure between these two MOFs, it was determined that the Dual-site Sips model should be implemented to the tetraamine-appended  $\text{Mg}_2(\text{dobpdc})(3-4-3)$  MOF selected for this study.

In order to adapt the Dual-site Sips model to our MOF material, the FMINCON optimization routine in MATLAB was used. This routine minimized the difference between the experimental isotherm data points and the data predicted by the isotherm model to yield the best possible fit of the model to the experimental isotherms. A detailed explanation of the isotherm model equations and the optimization function can be found in the work by Hughes et al. (2021), from which this model was adapted. A set of 12 fit parameters resulted from this optimization, which were then used to adapt the equations for the Dual-site Sips isotherm model such that they defined the isotherm curves of the tetraamine-appended

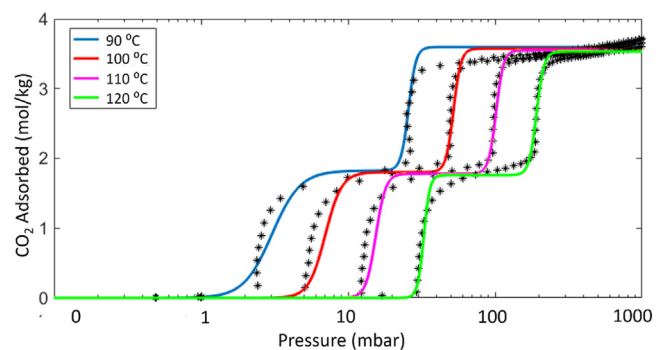


Fig. 3. The Dual-site Sips model was fitted to the experimental isotherm data of the tetraamine-appended  $\text{Mg}_2(\text{dobpdc})$  MOF material, where the experimental data is denoted by asterisks and the colored lines denote the model predictions.

MOF with acceptable accuracy (details presented in Supplementary Information, Tables SI1 & SI2).

Fig. 3 below compares the predictions of the optimized model to the experimental data, where the experimental data points are indicated by the asterisks, and the colored lines denote the isotherm curves predicted by the Dual-site Sips isotherm model. It can be seen that the Dual-site Sips isotherm model fits the experimental isotherm data for the tetraamine-appended  $\text{Mg}_2(\text{dobpdc})$  MOF material to an acceptable degree. Thus, we were able to use these fitted isotherm curves in our fixed bed adsorber model to predict the MOF's adsorption behavior. Note that the deviation between the model and experimental data at the top of the isotherms is due to experimental error, not modeling shortcomings (since isotherms are meant to asymptotically approach an upper limit, not continue to increase).

### 2.2. Fixed bed adsorber model

The MOF fixed bed adsorber system was modeled using Aspen Adsorption™ and was adapted from a similar model developed by Hughes et al. (2021). The MOF fixed bed adsorber model is represented by the flow diagram shown in Fig. 4. The adsorber vessel in this model is a cylindrical-shaped, fixed bed packed with spherical, tetraamine-appended  $\text{Mg}_2(\text{dobpdc})$  MOF particles with radii of approximately 0.2625 mm. Fixed bed adsorbers are chosen to reduce the bed size and the attrition of particles, while taking care to limit the pressure drop across the beds. One adsorber bed is modeled undergoing adsorption & desorption cycles, the results of which will be multiplied to scale up because in reality, several beds would be operating simultaneously. The number and the dimension of the beds, as well as the conditions within the adsorber (e.g., temperature, pressure, flow rate) are presented later in this paper.

The adsorber bed needs to be heated and cooled in order for the MOF material to complete the temperature swing regeneration process. The heating and cooling of the beds were achieved by internal heat exchangers that use water as the heat transfer medium, while the system outer boundaries were modeled as adiabatic. During the adsorption process, the heat exchanger maintained the bed temperature at 50 °C. During the desorption process, the heat exchanger rapidly raised the bed temperature using water at 150 °C passing at 275 kg/s within the heat exchanger. Once the MOF material desorption process was completed, the bed was cooled back down from 150 °C to 50 °C using a water flow rate of 500 kg/s at 50 °C. The internal heat exchangers were shell-and-tube exchangers with a tube diameter of 1 inch and pitch of 0.04 m. The heat transfer coefficient for the in-built heat exchanger within the fixed bed adsorber was given by an equation derived by Penny et al. (2010):

$$\frac{h_{HX} d_t}{k_{eff}} = \left( 0.333 + 0.26 Re_{d_t}^{0.533} \right) Pr^{0.33} \left( \frac{d_t}{d_p} \right)^{0.1} \quad (1)$$



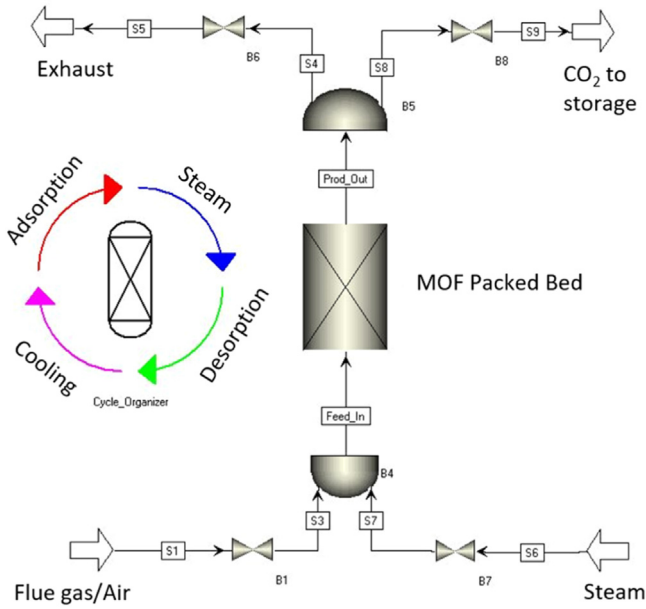


Fig. 4. Flow diagram of MOF fixed bed adsorber model developed in Aspen Adsorption™. The model is of a single packed bed of MOF solid sorbent pellets, and cycles between adsorption, steam pre-heating, steam desorption and cooling. The MOF packed bed is one dimensional in the flow direction with Node 1 at the bottom and the final node at the top.

where  $h_{HX}$  is the heat transfer coefficient,  $d_i$  is the heat exchanger tube diameter,  $k_{eff}$  is the effective thermal conductivity,  $Pr$  is the Prandtl number,  $d_p$  is the sorbent particle diameter, and the Reynolds number is given by  $Re_{d_i} = \frac{d_i \rho_g v_g}{\mu_g}$ .

It was shown in previous work that the direct steam injection lowers the desorption temperature (Kim et al., 2020). Hence direct steam, which is extracted from the NGCC power plant, is injected to the adsorber during the desorption step. The heat needed for regeneration is mainly provided by the embedded heat exchanger, not by the injected direct steam that mainly helps to reduce the partial pressure of  $CO_2$  in the bed thus improving regeneration. If steam gets condensed in the bed, it can cause the solid to form lumps and eventually to form slurry and therefore steam condensation in the bed is undesired. It should be noted that the temperature of the bed during regeneration remains much above the steam condensation temperature. The dual-site Sips isotherm model was incorporated into the fixed bed adsorber model using Aspen Custom Modeler. With the help of the cycle organizer feature in Aspen Adsorption™, the adsorber bed model was designed to continuously cycle through a 4-step process: adsorption, steam pre-heating, desorption, and cooling. Adsorption was set to occur until the bed was fully saturated with  $CO_2$ , followed by steam entering the bed for 120 s. Desorption was specified to continue until the average concentration of  $CO_2$  in the bed decreased to 0.25 mol/kg. Finally, the cooling step used the heat exchangers to bring the bed temperature back down to 50 °C.

Mass transfer in the bed was modeled by considering linear driving force with the following mass transfer coefficients:

$$\frac{1}{k_{OC}} = \frac{r_p^2}{15\epsilon_p D_{eff}} + \frac{1}{k_{chem}} \quad (2)$$

$$\frac{1}{k_{OP}} = \frac{r_p^2}{15D_{eff}} + \frac{1}{k_{phys}} \quad (3)$$

where  $k_{OC}$  and  $k_{OP}$  are the overall mass transfer coefficients for chemisorption and physisorption, respectively,  $r_p$  is the sorbent particle radius, which is 0.2625 mm, and  $D_{eff}$  is the effective particle diffusion given by  $D_{eff} = C_1(T_S)^{0.5}$ , where  $C_1$  is a constant and

$T_S$  is the temperature [K]. The value of  $C_1$  is the same value used in Hughes et al. (2021) since the diamine-appended MOF material used in their work was similar in structure and properties as the tetramine-appended MOF studied in this work. In the work of Hughes et al. (2021),  $C_1$  was optimally estimated by using experimental breakthrough data.

The parameters  $k_{chem}$  and  $k_{phys}$  are the mass transfer coefficients for chemisorption and physisorption given by

$$k_{chem} = k_{chem,0} \exp\left[\frac{-E_{chem}}{RT_0}\left(\frac{T_0}{T} - 1\right)\right] \quad (4)$$

$$k_{phys} = k_{phys,0} \exp\left[\frac{-E_{phys}}{RT_0}\left(\frac{T_0}{T} - 1\right)\right] \quad (5)$$

where  $k_{chem,0}$ ,  $k_{phys,0}$ ,  $E_{chem}$  and  $E_{phys}$  are fitted parameters,  $R$  is the ideal gas constant,  $T_0$  is the reference temperature (285 K for our model), and  $T$  is the operating temperature (Hughes et al., 2021). The value of the fitting parameters,  $k_{chem,0}$ ,  $k_{phys,0}$ ,  $E_{chem}$  and  $E_{phys}$ , is the same as in Hughes et al. (2021), where these parameters were optimally estimated by using the experimental thermogravimetric analysis data for the powdered material (so the first term on the right hand side of Eqs. (3) and (4) were neglected). The  $CO_2$  adsorption rate can be expressed as the summation of the chemisorption and physisorption rates:

$$\frac{dq_{CO_2}}{dt} = k_{chem}(q_{chem}^* - q_{chem}) + k_{phys}(q_{phys}^* - q_{phys}) \quad (6)$$

where  $q_{chem}$  and  $q_{phys}$  are chemisorption and physisorption loadings, respectively, and  $q_{chem}^*$  and  $q_{phys}^*$  are predicted loadings at equilibrium given by the dual-site Sips model.

The Ergun equation was used to determine the pressure drop across the adsorber bed using a bed voidage of 0.68 and a particle diameter of 0.525 mm. The equation for calculating the  $CO_2$  capture rate of the adsorber bed is:

$$Adsorber \ CO_2 \ capture \ rate = \text{mean} \left( \frac{(N_{CO_2})_{in,ads} - (N_{CO_2})_{out,ads}}{(N_{CO_2})_{in,ads}} \right) \times 100\% \quad (7)$$

where  $(N_{CO_2})_{in,ads}$  is the flow rate of  $CO_2$  into the adsorber bed [mol/s] and  $(N_{CO_2})_{out,ads}$  is the flow rate of  $CO_2$  out of the adsorber bed [mol/s]. The time-average of the terms in parentheses is taken over the adsorption cycle to obtain the mean  $CO_2$  capture rate over the entire adsorption process. For example, the mean of  $(N_{CO_2})_{in,ads}$  would equal the flow rate of the inlet gas time-averaged over the adsorption cycle. Although the inputs to Eq. (7) are for a single adsorber bed, the resulting  $CO_2$  capture rate holds true for the entire solid sorbent system, which consists of multiple identical adsorber beds in parallel.

The carbon capture rate for the entire hybrid (membrane + solid sorbent) system is given by:

$$Overall \ CO_2 \ capture \ rate = \text{mean} \left( \frac{(N_{CO_2})_{in,mem} - (N_{CO_2})_{out,ads}}{(N_{CO_2})_{in,mem}} \right) \times 100\% \quad (10)$$

where  $(N_{CO_2})_{in,mem}$  is the flow rate of  $CO_2$  from the NGCC exhaust into the membrane system [mol/s] and  $(N_{CO_2})_{out,ads}$  is the flow-rate of  $CO_2$  out of the adsorber bed [mol/s]. The time-average of the terms in the parentheses is taken over the adsorption cycle to obtain the mean  $CO_2$  capture rate over the entire adsorption process. Net-zero operation occurs when Eq. (10) gives 100 % and net-negative operation occurs when Eq. (10) exceeds 100 % (which can only occur when less than 400 ppm  $CO_2$  exists in the adsorber outlet stream). Note that the  $CO_2$  that enters the carbon capture systems via air is subtracted off from inlet stream terms-  $(N_{CO_2})_{in,mem}$  and  $(N_{CO_2})_{in,ads}$  to ensure that 100 % capture is attained when the outlet exhaust stream has 400 ppm  $CO_2$ .

**Table 1**

Fixed parameters for the simulations performed on the fixed bed adsorber in this section. Bed height, bed voidage, particle diameter and bulk sorbent density values have been taken from Hughes et al. (Kundu et al., 2018).

| Parameter                      | Value  | Units                  |
|--------------------------------|--------|------------------------|
| Bed Height, h                  | 10     | m                      |
| Bed Voidage, $\epsilon$        | 0.68   | -                      |
| MOF Particle Diameter, $d_p$   | 525    | $\mu\text{m}$          |
| Bulk Sorbent Density, $\rho_s$ | 315.35 | $\text{kg}/\text{m}^3$ |
| Adsorption Bed Temperature     | 50     | $^{\circ}\text{C}$     |
| Desorption Bed Temperature     | 150    | $^{\circ}\text{C}$     |
| Inlet Gas Temperature          | 30     | $^{\circ}\text{C}$     |
| Steam Temperature              | 139.85 | $^{\circ}\text{C}$     |
| Steam Pressure                 | 1.5    | bar                    |

A key assumption made in this model is that the adsorption behavior of the tetraamine-appended  $\text{Mg}_2(\text{dobpdc})$  MOF material does not change significantly with a shift to lower operating temperatures. The experimental isotherm data collected for the MOF material ranged from 90 to 120  $^{\circ}\text{C}$ , while the adsorber beds in this carbon capture system would ideally operate between 50 and 150  $^{\circ}\text{C}$ . In order to extrapolate these isotherms to these temperatures, we assumed that the general shape of the isotherm curves remained unchanged.<sup>1</sup> We also assumed that the linear driving force kinetic model used by Hughes et al. (Kundu et al., 2018) could be applied to this MOF since the MOF material used in their work was similar in structure and properties. Similar to the work of Hughes et al. (2021), it was assumed that  $\text{CO}_2$  is the only gas species to be significantly adsorbed by the MOF sorbent used in this system since the tetraamine-appended MOF was shown to be highly selective for  $\text{CO}_2$  (Sinha et al., 2017, Kim et al., 2020).

### 3. Results and discussion

In this section, the optimal sorbent bed conditions are first determined through a series of simulations where parameters are changed over a range to find the best performance (Section 3.1). Mode 1 & 2 simulations are then performed using this optimal bed design to determine key outputs such as cycle times and  $\text{CO}_2$  capture rates (Section 3.2). Finally, ambient air is added to the Mode 2 bed at varying flow rates to determine how excess air impacts bed performance (Section 3.3).

#### 3.1. Parametric variations

Parametric variations were run in order to determine the ideal conditions that would result in the highest  $\text{CO}_2$  bed loadings, shortest cycle times, and lowest costs. Table 1 lists some of the fixed parameters used in these simulations, some of which have been adopted from Hughes et al.'s work (Hughes et al., 2021) due to the similarities of the MOF sorbents used. The bed adsorption and desorption temperatures were selected based on the isotherms and operating bounds of the MOF selected for this study (Kim et al., 2020). The three variable input parameters that are studied here are: bed diameter and number of beds (Section 3.1.1), adsorber inlet gas pressure (Section 3.1.2), and steam flow rate (Section 3.1.3). A summary of the final values selected for these variable input parameters is given at the end of this section in Table 2.

##### 3.1.1. Bed diameter and number of beds

The influence of the adsorber bed diameter and the number of beds on pressure drop is investigated here to determine the minimal number and size of adsorber beds needed to maintain a reasonable pressure

<sup>1</sup> This assumption has been backed by Dr. Long's group through verbal communication, who are also planning to publish data for isotherms at a lower temperature range in the near future.

**Table 2**

Summary of values selected for input parameters varied in this section.

| Parameter                   | Selected Value | Units                  |
|-----------------------------|----------------|------------------------|
| Adsorber Inlet Gas Pressure | 4.9*           | bar                    |
| Steam flow rate             | 0.15           | $\text{kmol}/\text{s}$ |
| Adsorber Bed Number         | 10             | -                      |
| Bed Diameter                | 5              | m                      |

\* Although the parametric studies resulted in 5.0 bar for the adsorber inlet gas pressure, about 0.1 bar was lost in the piping from the blowers to the adsorber bed inlet in our Aspen flow-sheet, resulting in an actual inlet pressure of 4.9 bar to the adsorber beds.

drop. Fig. 5 shows the effects of changing the bed diameter and the number of beds on the pressure drop across the beds. In Fig. 5A, we fixed the number of adsorber beds to 10 and varied the bed diameter. As expected, pressure drop decreases significantly with respect to bed diameter, since pressure drop is proportional to gas velocity squared as shown in Eq. (8), and gas velocity is inversely proportional to bed diameter squared for a fixed flow rate:  $v_g = Q/(\pi D^2/4)$ . We selected 5 m as the bed diameter based on these results because it is the smallest diameter that results in a pressure drop equal to 0.2 bars. Once we fixed the bed diameter to 5 m, we varied the number of adsorber beds (Fig. 5B). We decided to proceed with 10 adsorber beds based on these results because increasing the number of beds beyond 10 would result in excess capital cost with minimal operating cost gain (since pressure drop is already pretty low at 10 beds). Note that there would need to be more than 10 fixed beds total for our system since 10 are allocated for adsorption at a given time. Therefore, a few more beds will be needed to undergo the pre-heating, desorption and cooling steps in addition to the 10 beds undergoing adsorption. The exact number of total beds will be determined later in this paper.

##### 3.1.2. Adsorber inlet pressure

Although pressurizing gas is typically not worth the added operating cost in traditional carbon capture systems, we have a unique design where excess electricity is available to our carbon capture system during off-peak NGCC operation (Mode 2). Therefore, pressurizing the inlet gas stream to our adsorber system could be beneficial in this application since the electricity is essentially "free" to the carbon capture system. The effect of inlet gas pressure on  $\text{CO}_2$  loading capacity was observed by running the fixed bed simulation at pressures ranging between 1.5 and 7.5 bars. It can be seen from Fig. 6A that the average  $\text{CO}_2$  loading in the bed increases with respect to inlet pressure. Increasing the pressure from 2.5 bars to 5 bars, for example, increases the average bed loading from 1.55 mol/kg to 2.37 mol/kg, which is a ~150 % increase in loading for doubling the pressure.

The effect of adsorber inlet gas pressure on cycle time also appears to be significant. The cycle time changes from 149 to 192 min for a climb from 2.5 to 5 bars, which is a ~130 % change in cycle time for doubling the adsorber inlet gas pressure. Since the inlet pressure significantly affects both the average bed loading and the cycle time, it is essential to determine and set a value for the inlet pressure which will create a balance between the two numbers. Observations seemed to suggest that specifying the adsorber inlet pressure to 5 bars provides a balanced value that maximizes the bed loading and minimizes the cycle time at the same time. Therefore, 5.0 bars was selected as the adsorber gas inlet pressure (as indicated by the vertical dashed line in Fig. 6A).

##### 3.1.3. Desorption steam flow rate

The effect of steam flow rate on regeneration (desorption + cooling) time is investigated in this section. All other parameters were kept constant (e.g. steam temperature, composition, pressure, etc). Fig. 6B shows that increasing the steam flow rate leads to a significant drop

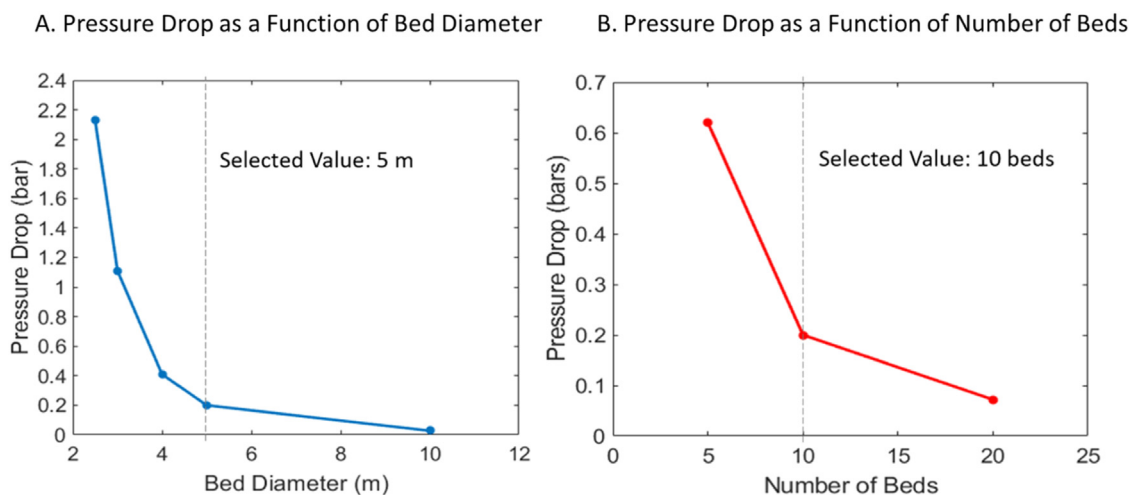


**Fig. 5.** (A) Pressure drop as a function of bed diameter (assuming 10 parallel adsorber beds), and (B) pressure drop as a function of number of adsorber beds (assuming a 5 m diameter for each bed). Based on these results, 10 parallel adsorber beds of 5 m diameter were selected to minimize pressure drop without making the system excessively large or expensive.

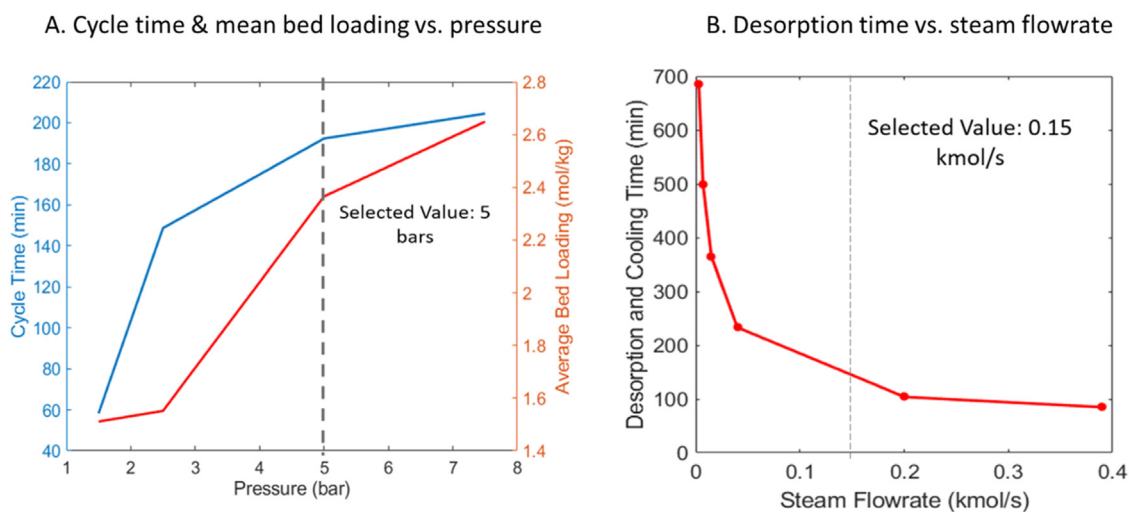


**Fig. 6.** (A) Bed cycle time (left y-axis, blue) and average  $\text{CO}_2$  bed loading (right y-axis, red) as a function of inlet gas pressure. Both bed loading and cycle time increase with respect to inlet gas pressure. (B) Desorption and cooling (regeneration) time as a function of steam flow rate. Regeneration time decreases with increasing steam flow rate, and 0.15 kmol/s was selected as an ideal steam flow rate moving forward.

in regeneration time, with a steep initial drop-off as steam flow rate approaches zero. The maximum practical limit for steam flow rate that could reasonably be extracted from our NGCC plant was 0.15 kmol/s (as indicated by the vertical dashed line in Fig. 6B), so we selected that as our fixed value. This value results in reasonably low regeneration times (~150 min).

### 3.1.4. Parameter variation results

The values we selected for the variable input parameters (varied in Sections 3.1.1–3.1.3) are summarized in Table 2. These values, in addition to the fixed values listed in Table 1, will serve as model inputs for the rest of the simulation results presented in this paper, unless otherwise stated.

## 3.2. Bed performance in modes 1 & 2

Now that the adsorber bed design has been defined (Section 3.1), we will use the selected input values (listed in Table 2) along with the fixed input values (listed in Table 1) to simulate our system under NGCC hybrid conditions. More specifically, we will run our sorbent bed model

in both Mode 1 & Mode 2 (as shown in Fig. 1) to determine how it will perform under these conditions. The only inputs to our model that vary between Modes 1 & 2 are the adsorber inlet gas flow rate and mole fractions (compared in Table 3). In Mode 1, the inlet gas feed is purely membrane carbon capture exhaust, whereas in Mode 2, the inlet gas feed is a mixture of membrane exhaust, compressed air off the NGCC compressor and pressurized ambient air drawn in from the surroundings. As seen in Table 3, the inlet gas flow rate increases and the mole fractions change when transitioning from Mode 1 to Mode 2 because of the addition of air streams. These values were obtained by running a complex optimization on the integrated NGCC + membrane + solid sorbent system as described in Section S3 of the Supplementary Information and in another publication by our team (Soeppan et al., 2024).

Fig. 7 shows the  $\text{CO}_2$  loading profiles for Mode 1, where the five colored loading curves shown correspond to five locations in the bed: inlet (Node 1), close to inlet (Node 10), middle of bed (Node 40), close to outlet (Node 70) and outlet (Node 80). These nodes were selected to understand how  $\text{CO}_2$  loading vs. time varies at different bed locations. As expected, nodes closer to the inlet load with  $\text{CO}_2$  earlier than nodes closer to the outlet. Furthermore, it can be seen that the nodes near the

**Table 3**  
Inlet gas stream conditions for Mode 1 & Mode 2 simulations.

| Input Gas Parameters                     | Mode 1                 | Mode 2  |
|--|------------------------|---|
| Inlet Gas CO <sub>2</sub> mole fraction  | 0.0132                 | 0.0115  |
| Inlet Gas H <sub>2</sub> O mole fraction | 0.0611                 | 0.0787  |
| Inlet Gas N <sub>2</sub> mole fraction   | 0.7942                 | 0.8764  |
| Inlet Gas O <sub>2</sub> mole fraction   | 0.1315                 | 0.0334  |
| Inlet Gas Molar Flow Rate, kmol/s        | 0.9158                 | 1.382   |
| Source(s) of gas                         | 100 % membrane exhaust | 97.98 % membrane exhaust<br>1.42 % compressed air<br>0.60 % ambient air |

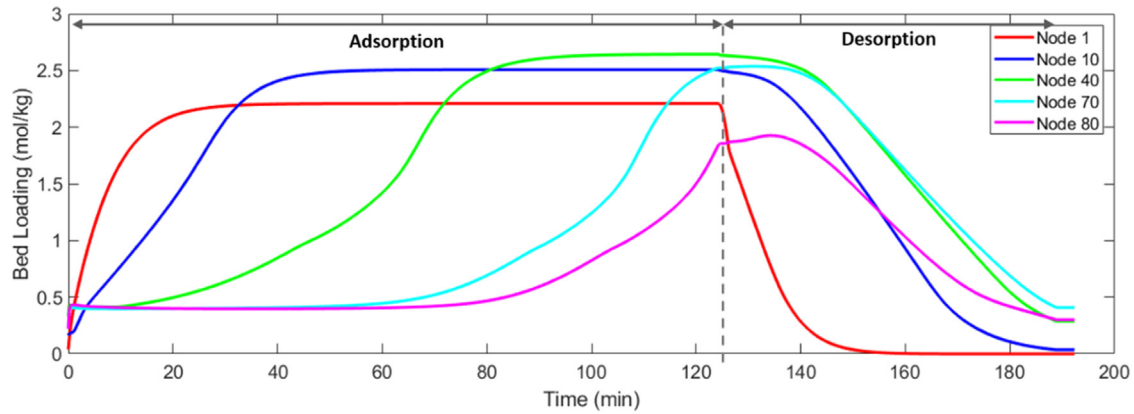


**Fig. 7.** MOF CO<sub>2</sub> loading vs. time in a fixed bed adsorber for Mode 1 operation (NGCC power plant sending electricity to the grid). Bed loading is shown for five different nodes in the model: Node 1 (inlet node), Node 10 (close to inlet), Node 40 (node half-way through the bed), Node 70 (close to outlet), and Node 80 (outlet node). Total cycle time is 192.33 min: 124.5 min for adsorption + 64.5 min for desorption + 3.33 min for cooling.

**Table 4**  
Key results for Modes 1 & 2: required power and heat, and carbon capture rates.

|   | Mode 1  | Mode 2 |
|---|---------|--------|
| <b>Energy Flows</b>                                 |         |        |
| NGCC Gross Power [MW]                               | 641     | 635    |
| NGCC Net Power [MW]                                 | 344     | 175    |
| Power to compress gas entering adsorber system [MW] | 70.27   | 200.64 |
| Cooling duty of packed beds [GJ/hr]                 | 1059.68 | 869.19 |
| <b>Carbon Capture Rates</b>                         |         |        |
| Solid Sorbent System                                | 86.6 %  | 85.4 % |
| Membrane System                                     | 88.8 %  | 92.6 % |
| Overall Carbon Capture System                       | 98.4 %  | 98.9 % |

middle of the bed have higher final CO<sub>2</sub> loadings than the nodes at the inlet and outlet. This may be explained by the fact that the inlet gas stream enters the bed at 30 °C and takes awhile to reach the bed temperature of 50 °C. Bed loading at the outlet (Node 80) is lower due to pressure drop and reduced CO<sub>2</sub> partial pressure at the end of the bed. During the Mode 1 cycle, 124.5 min are required for adsorption and 67.83 min are required for regeneration. Since the ratio of adsorption time to regeneration time is roughly 2:1 and we have 10 beds for adsorption, we would need to dedicate 5 more beds to regeneration (bringing the total number of system beds up to 15). This system design is depicted in Fig. 9. The carbon capture rate of this adsorber system during Mode 1 operation 86.6 % based on Eq. (9). When this system is combined with the membrane carbon capture system upstream, this results in a high overall carbon capture rate of 98.4 % during Mode 1. These results are summarized along with Mode 2 carbon capture rates in Table 4.

Mode 2 operation involved CO<sub>2</sub> adsorption from the membrane-based CCS system exhaust from the compressed air redirected from the NGCC power plant, and ambient air from the surroundings. Membrane exhaust accounts for 97.98 % of the total input flow rate to the system,

while compressed air from the NGCC plant accounts for 1.42 % and ambient air accounts for 0.60 %. The membrane exhaust (1,641,007 kg/hr) is determined by the flow rate of gases exiting the NGCC plant, the other percentages were limited by the amount of compressed air that could be drawn out from the NGCC plant (approximately 23,809 kg/hr) as well as from ambient air (10,000 kg/hr). As depicted in Fig. 8, total cycle time during Mode 2 is approximately 160.67 min, with 96.33 min spent in adsorption and 64.34 min spent in regeneration. Mode 2 has a lower cycle time than Mode 1 because of the higher gas flow rate caused by the additional air streams. The ratio of adsorption to regeneration time can be rounded up to 2:1 for Mode 2 as well, meaning that the system design shown in Fig. 9 (10 beds for adsorption + 5 beds for desorption) should work well for both modes. The carbon capture rate for the solid sorbent system during Mode 2 was found to be 85.4 %, and the overall carbon capture rate of the membrane + solid sorbent system in Mode 2 was 98.9 %. These results are summarized along with the Mode 1 carbon capture results in Table 4. These results indicate that our hybrid system is capable of attaining near net-zero conditions. The system could theoretically approach net-zero or net-negative conditions if more ambient air were added to the mix, as explored in the next section. Heat and power inputs to the system in Mode 1 & 2 operation are also listed in Table 4. The power input in Mode 2 is higher because air has to be moved and pressurized in addition to moving the membrane exhaust. This results in a lower net power for Mode 2. However, this cut in gross power is okay during Mode 2 operation, when there's less demand for electricity on the grid.

### 3.3. Effect of adding excess ambient air in mode 2

In Section 3.2, we demonstrated that 98–99 % overall carbon capture rate is possible for our hybrid system. However, our system could theoretically attain 100+% rate (negative emissions) if it were able to remove enough CO<sub>2</sub> from air during Mode 2 to offset any CO<sub>2</sub> emitted



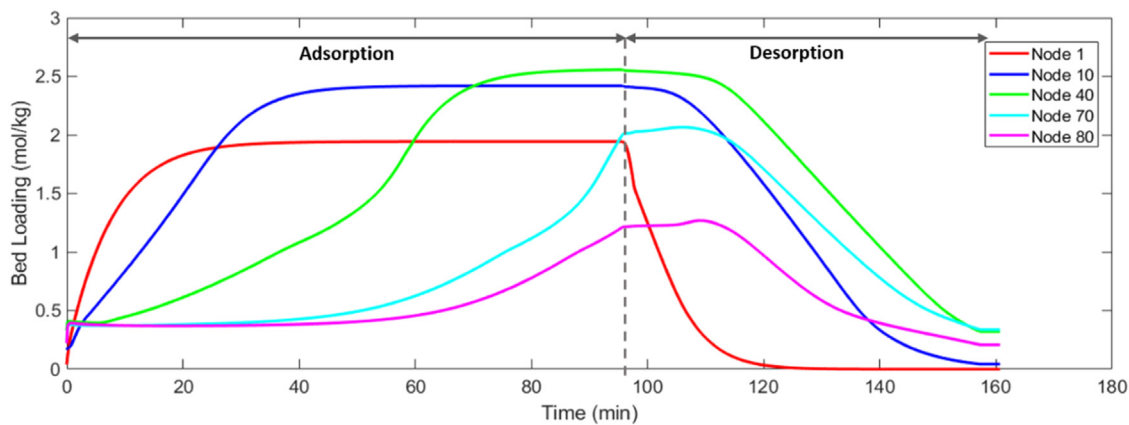


**Fig. 8.** CO<sub>2</sub> loading in the MOF adsorber bed vs. time for Mode 2 operation (adsorber processes air in addition to membrane exhaust). Bed loading is shown for five different nodes in the model: Node 1 (inlet node), Node 10 (close to inlet), Node 40 (node half-way through the bed), Node 70 (close to outlet) and Node 80 (outlet node). Total cycle time is 160.67 min: 96.33 min for adsorption + 61 min for desorption + 3.34 min for cooling.

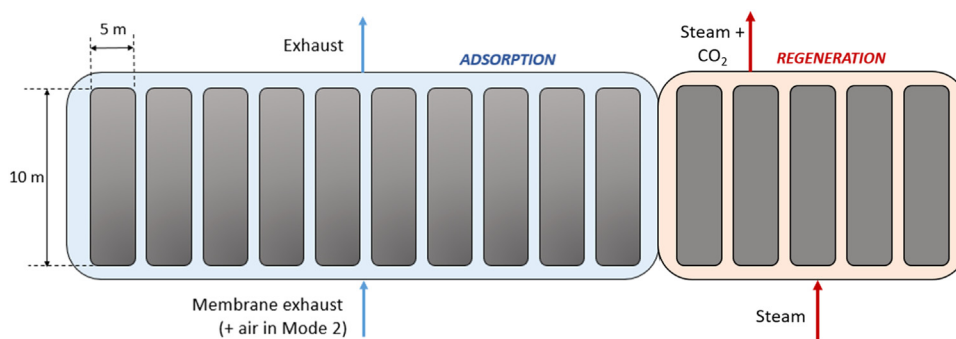


**Fig. 9.** Design of solid sorbent carbon capture system, which consists of 15 beds (5 m diameter, 10 m height) filled with MOF solid sorbent spheres. 10 beds are undergoing adsorption from the membrane exhaust (mixed with air for Mode 2) at a given time, while 5 beds are undergoing steam regeneration. The beds remain fixed in space while the membrane exhaust and steam get routed to different beds on a timer.

during Mode 1. In Section 3.2, we assumed that the air input to the adsorber beds was 10,000 kg/hr pressurized ambient air and 23,809 kg/hr compressed air siphoned off the NGCC compressor. In this section, we study the effect of supplementing that stream with excess ambient air drawn in from the surroundings during Mode 2. To study the impact of excess ambient air on bed performance, we added ambient air in quantities such that 8 %, 30 % and 45 % of the inlet gas stream entering the adsorber bed consisted of ambient air, respectively.

Fig. 10 shows the CO<sub>2</sub> loading of an average bed node (Node 40) vs. time for each of these air cases. The bed loadings for 8 %, 30 % and 45 % excess ambient air are shown in comparison to 0.6 % ambient air, which was the amount added for Mode 2 operation. Two trends are clear from Fig. 10: (1) cycle time decreases as more air is added, and (2) CO<sub>2</sub> loading decreases as more air is added. These trends are correlated because cycle time decreases as a result of the bed reaching (lower) capacity sooner. The decrease in CO<sub>2</sub> loading with excess air is undesirable since the goal is to capture more CO<sub>2</sub> in order to reach negative emissions. However, the trend also makes sense because flooding the inlet stream with air lowers the partial pressure of CO<sub>2</sub> in the mixture, resulting in lower CO<sub>2</sub> capacity in the sorbent. Ultimately, the results in Fig. 10 demonstrate that the MOF sorbent selected for our model performs worse under DAC conditions. Future work in this area should consider solid sorbents that are better suited for DAC than the one selected for this study.

#### 4. Conclusions

This work consisted of designing and optimizing the performance of a MOF fixed bed adsorber system coupled to an NGCC power plant and upstream membrane carbon capture system. The purpose of this fixed bed adsorber system is to capture excess CO<sub>2</sub> from the membrane exhaust during normal operation and to capture additional CO<sub>2</sub> from the

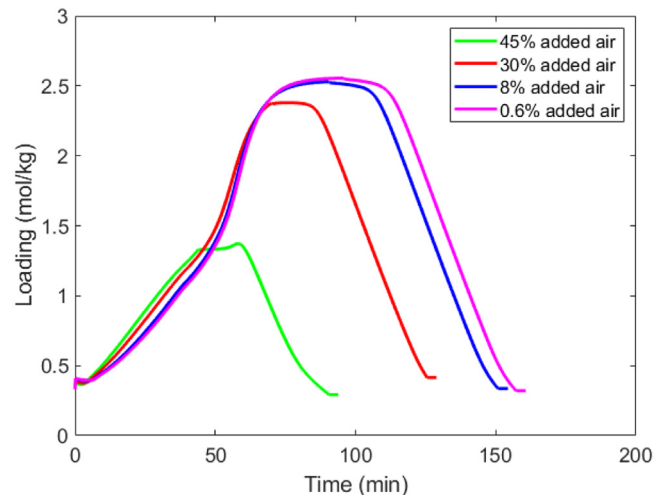


**Fig. 10.** CO<sub>2</sub> bed loading at the middle of the bed (Node 40) as a function of time for four cases: added air in Mode 2 (0.6 %), 8 % added air, 30 % added air, and 45 % added air (where air is added to the adsorber bed inlet stream). CO<sub>2</sub> loading and cycle time decrease as more air is added because the lower partial pressure of CO<sub>2</sub> in the mixture reduces sorbent performance.

air during off-peak hours. This novel hybrid carbon capture system could theoretically attain net-zero or net-negative CO<sub>2</sub> footprints for natural gas plants in the future by using CO<sub>2</sub> captured from air to offset any CO<sub>2</sub> emissions. However, we were unable to reach net-zero or net-negative emissions in this study due to limitations in our solid sorbent selection and in the amount of compressed air that could be tapped from the com-



pressor. However, our modeled fixed bed adsorber system was able to attain carbon capture rates of 86.6 % and 85.4 % (for Modes 1 & 2), which correspond to overall capture rates of 98.4 % and 98.9 % (for Modes 1 & 2) when combined with the membrane carbon capture system. These results indicate that our hybrid carbon capture system is capable of approaching a net-zero CO<sub>2</sub> footprint for an NGCC power plant. Future research should be conducted on alternate solid sorbents that are better suited for direct air capture so that higher volumes of air can be processed, enabling this system to achieve net-zero or net-negative CO<sub>2</sub> emissions. Future work should also explore the techno-economic benefits of coupling direct air capture technology with natural gas infrastructure. By leveraging the steam, electricity and compressed air of NGCC plants, direct air capture operating costs could be significantly reduced.

## Funding

This research was supported by ARPA-E under the program titled Flexible Carbon Capture and Storage (FLECCS)-Phase 1 (grant number DE-AR0001308).

## Acknowledgments

The authors would like to thank Dr. Jeffrey R. Long and Dr. Eugene J. Kim, from the University of California, Berkeley, for their guidance, advice, and invaluable feedback regarding the MOF modeled in this paper.

## Supplementary materials

Supplementary material associated with this article can be found, in the online version, at [doi:10.1016/j.ccst.2023.100170](https://doi.org/10.1016/j.ccst.2023.100170).

## References

- Abudu, K., Igie, U., Minervino, O., Hamilton, R., 2020. Gas turbine minimum environmental load extension with compressed air extraction for storage. *Appl. Thermal Eng.* 180, 115869.
- G. Alptekin, "Membrane-sorbent hybrid system for post-combustion carbon capture," Nov. 2020.
- Baker, R.W., Freeman, B., Kniep, J., Wei, X., Merkel, T., 2017. CO<sub>2</sub> capture from natural gas power plants using selective exhaust gas recycle membrane designs. *Int. J. Greenh. Gas Control* 66, 35–47.
- Bao, Z., Yu, L., Ren, Q., Lu, X., Deng, S., 2011. Adsorption of CO<sub>2</sub> and CH<sub>4</sub> on a magnesium-based metal organic framework. *J. Colloid Interface Sci.* 353 (2), 549–556.
- Choi, S., Drese, J.H., Eisenberger, P.M., Jones, C.W., 2011. Application of amine-tethered solid sorbents for direct CO<sub>2</sub> capture from the ambient air. *Environ. Sci. Technol.* 45 (6), 2420–2427.
- Diego, M.E., Bellas, J.M., Pourkashanian, M., 2018. Techno-economic analysis of a hybrid CO<sub>2</sub> capture system for natural gas combined cycles with selective exhaust gas recirculation. *Appl. Energy* 215 (February), 778–791.
- Gribble, D., et al., 2022. Demo-scale testing of a hybrid membrane-sorbent system for post-combustion CO<sub>2</sub> capture. *SSRN Electron. J.*
- Hansen, J., Ruedy, R., Sato, M., Lo, K., 2010. Global surface temperature change. *Rev. Geophys.* 48 (4), 1–29.
- Hashemi, S.M., Sedghkarder, M.H., Mahinpey, N., 2022. Calcium looping carbon capture: progress and prospects. *Can. J. Chem. Eng.* 100 (9), 2140–2171.
- He, Z., Ricardez-Sandoval, L.A., 2016. Dynamic modelling of a commercial-scale CO<sub>2</sub> capture plant integrated with a natural gas combined cycle (NGCC) power plant. *Int. J. Greenh. Gas Control* 55, 23–35.
- Hefti, M., Joss, L., Bjelobrk, Z., Mazzotti, M., 2016. On the potential of phase-change adsorbents for CO<sub>2</sub> capture by temperature swing adsorption. *Faraday Discuss* 192 (0), 153–179.
- Hughes, R., et al., 2021. Isotherm, kinetic, process modeling, and techno-economic analysis of a diamine-appended metal-organic framework for CO<sub>2</sub> capture using fixed bed contactors. *Energy Fuels* 35 (7), 6040–6055.
- Igie, U., Abbondanza, M., Szymański, A., Nikolaidis, T., 2021. Impact of compressed air energy storage demands on gas turbine performance. *proceedings of the institution of mechanical engineers. Part A J. Power Energy* 235 (4), 850–865.
- Keith, D.W., Holmes, G., St. Angelo, D., Heidel, K., 2018. A process for capturing CO<sub>2</sub> from the atmosphere. *Joule* 2 (8), 1573–1594.
- Kiani, A., Jiang, K., Feron, P., 2020. Techno-economic assessment for CO<sub>2</sub> capture from air using a conventional liquid-based absorption process. *Front. Energy Res.* 8 (May), 1–13.
- Kim, E.J., et al., 2020. Cooperative carbon capture and steam regeneration with tetraamine-appended metal-organic frameworks. *Science* 369 (6502), 392–396.
- Kundu, J., Stilck, J.F., Lee, J.H., Neaton, J.B., Prendergast, D., Whitelam, S., 2018. Cooperative gas adsorption without a phase transition in metal-organic frameworks. *Phys. Rev. Lett.* 121 (1), 015701.
- Lackner, K.S., Brennan, S., Matter, J.M., Park, A.H.A., Wright, A., Van Der Zwaan, B., 2012. The urgency of the development of CO<sub>2</sub> capture from ambient air. *Proc. Natl. Acad. Sci. U. S. A.* 109 (33), 13156–13162.
- Lenzen, N.J.L., et al., 2019. Improvements in the GISTEMP uncertainty model. *J. Geophys. Res. Atmos.* 124 (12), 6307–6326.
- Li, J.R., Kuppler, R.J., Zhou, H.C., 2009. Selective gas adsorption and separation in metal-organic frameworks. *Chem. Soc. Rev.* 38 (5), 1477–1504.
- McDonald, T.M., Lee, W.R., Mason, J.A., Wiers, B.M., Hong, C.S., Long, J.R., 2012. Capture of carbon dioxide from air and flue gas in the alkylamine-appended metal-organic framework mmen-Mg<sub>2</sub>(dobpdc). *J. Am. Chem. Soc.* 134 (16), 7056–7065.
- Merkel, T.C., Lin, H., Wei, X., Baker, R., 2010. Power plant post-combustion carbon dioxide capture: an opportunity for membranes. *J. Memb. Sci.* 359 (1–2), 126–139.
- Merkel, T.C., Wei, X., He, Z., White, L.S., Wijmans, J.G., Baker, R.W., 2012. Selective exhaust gas recycle with membranes for CO<sub>2</sub> capture from natural gas combined cycle power plants. *Ind. Eng. Chem. Res.* 52 (3), 1150–1159.
- Millward, A.R., Yaghi, O.M., 2005. Metal-organic frameworks with exceptionally high capacity for storage of carbon dioxide at room temperature. *J. Am. Chem. Soc.* 127 (51), 17998–17999.
- Pai, K.N., Baboolal, J.D., Sharp, D.A., Rajendran, A., 2019. Evaluation of diamine-appended metal-organic frameworks for post-combustion CO<sub>2</sub> capture by vacuum swing adsorption. *Sep. Purif. Technol.* 211, 540–550.
- Penny, C., Naylor, D., Friedman, J., 2010. Heat transfer to small cylinders immersed in a packed bed. *Int. J. Heat Mass Transf.* 53 (23–24), 5183–5189.
- Realf, M., et al., 2021. Positive power with negative emissions: flexible NGCC enabled by modular direct air capture (DAC). In: *Proceedings of the AIChE Annual Meeting*.
- Sadiq, M.M., et al., 2020. A pilot-scale demonstration of mobile direct air capture using metal-organic frameworks. *Adv. Sustain. Syst.* 4 (12).
- Seipp, C.A., Williams, N.J., Kidder, M.K., Custelcean, R., 2017. CO<sub>2</sub> capture from ambient air by crystallization with a guanidine sorbent. *Angew. Chem.* 129 (4), 1062–1065.
- Sheha, M., Graham, E., Herzog, H., 2021. Steady state and dynamic modeling of a flexible carbon capture-equipped power plant integrated with lime-based direct air capture. In: *Proceedings of the AIChE Annual Meeting*.
- Shi, X., et al., 2020. Sorbents for the direct capture of CO<sub>2</sub> from ambient air. *Angew. Chem. Int. Ed.* 59 (18), 6984–7006.
- Siegelman, R.L., et al., 2019. Water enables efficient CO<sub>2</sub> capture from natural gas flue emissions in an oxidation-resistant diamine-appended metal-organic framework. *J. Am. Chem. Soc.* 141 (33), 13171–13186.
- Sinha, A., Darunte, L.A., Jones, C.W., Realf, M.J., Kawajiri, Y., 2017. Systems design and economic analysis of direct air capture of CO<sub>2</sub> through temperature vacuum swing adsorption using MIL-101(Cr)-PEI-800 and mmen-Mg<sub>2</sub>(dobpdc) MOF Adsorbents. *Ind. Eng. Chem. Res.* 56 (3), 750–764.
- Soeppan, B., Habib, M., Zhang, Z., Nemetz, L., Haque, M., Esquino, A., Rivero, J., Bhat-tacharyya, D., Lipscomb, G., Matuszewski, M., Hornbostel, K., 2024. Optimization of a natural gas power plant with membrane and solid sorbent carbon capture systems. *Carbon Capture Sci. Technol.* 10, 100165.
- Yang, C., Wang, P., Fan, K., Ma, X., 2020. Performance of gas turbine multi generation system regulated with compressor bypass extraction air energy storage. *Appl. Thermal Eng.* 172, 115181.